

論文

[2180] Microscopic Experimental Observation of Concrete

Junichiro NIWA * , *Ahmed M. FARAHAT* * and *Kouji YAMADA* *

1. INTRODUCTION

The idea of defining the inelastic behavior of different materials, independent of planes of different orientations within the material has a long history. For metals, in the slip theory of plasticity[1], the stresses acting on various slip planes are assumed to be the resolved components of the applied macroscopic stress tensor, while the plastic strains on the slip planes are not the resolved components of the macroscopic strain tensor. For concrete, in the microplane models[2][3], the strains on various planes are assumed to be resolved components of the macroscopic strain tensor while the stresses on these planes are not resolved components of the macroscopic stress tensor. However, because of the lack of microscopic experimental data, the material is assumed to be either statically or kinematically constrained. On the other hand, the authors believe that the real stress and strain fields at the microlevel are highly scattered and nonsmooth. Therefore, the effect of the nonuniform stress or strain distribution at the microlevel should be considered. Recently, although some investigators[3] tried to consider the nonuniformity of strain distribution in concrete, a more precise distribution of microstrains seems necessary.

In the current study, an experimental work is conducted to observe the real distribution of the microstrains in concrete. For this purpose, five specimens are examined. In these specimens, coarse aggregates are simulated by rounded steel cylinders of 3.2 cm diameter and 5.0 cm height, embedded in mortar. The rounded steel cylinders are used to provide an idealized smooth surface for measuring system. Finally, the effects of mortar strength, specimen size and measuring procedure(i.e. gauge length) on the distribution of the microstrains are investigated.

2. DESCRIPTION OF SPECIMENS

As shown in Fig.1, two different sizes of specimens are used. The smaller one has dimensions of 16.5 x 18 cm while the bigger one has dimensions of 20 x 18 cm. All specimens have the same thickness of 5 cm. From the macroscopic point of view, the difference of the selected sizes is not too much and the effect of specimen size may not be obtained. On the other hand, from the microscopic point of view, the arrangement of aggregates and the number of contacts in both sizes are different since the smaller size has one row less than that of the bigger size and may affect the results. As shown in Fig.1, specimens consist of rounded steel cylinders embedded in mortar. Since the effect of strength of mortar on the microstrain distribution is to be investigated, mortar with two different design strengths, which are 200 and 400 kgf/cm², are used. The mix proportions of the two types are shown in Table 1. Moreover, in Table 2, a complete description of all specimens(i.e. strength of mortar, gauge length, and size) is given.

* Department of Civil Engineering, Nagoya University

Table 1. Mix proportion of mortar

strength(kgf/cm ²)	unit weight(kg/m ³)		
	water	cement	sand
200	347	589	1196
400	239	685	1393

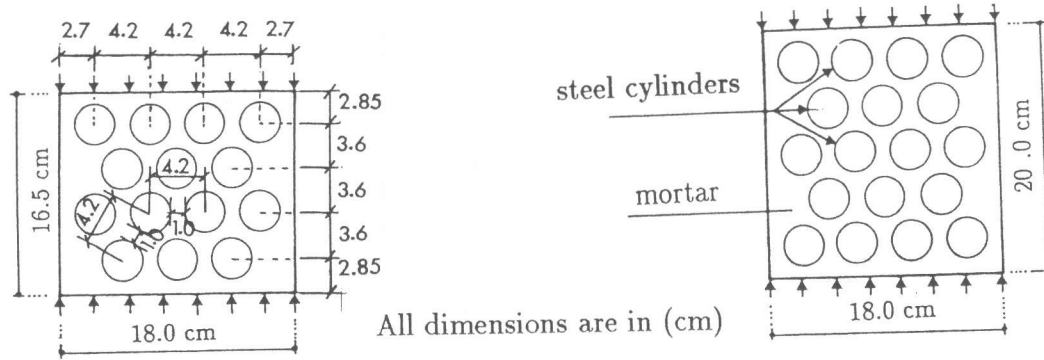


Fig. 1 The Main Features of Specimens

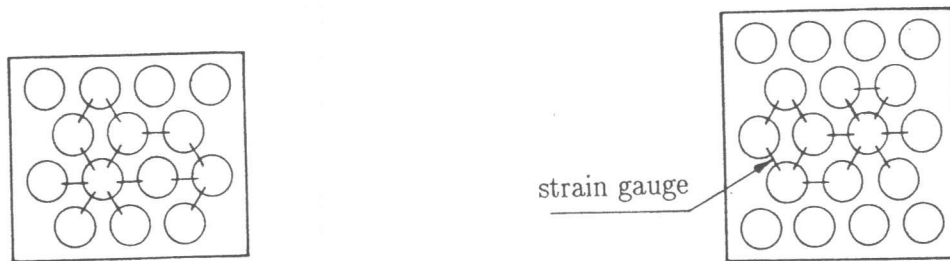


Fig. 2 Arrangement of Strain Gauges

Table 2. Strength of mortar, gauge length, and size of all specimens

specimen no.	strength(kgf/cm ²)	gauge length (mm)	size
1	314	10	big
2	314	30	big
3	606	30	big
4	314	10	small
5	606	10	small

3. MEASURING SYSTEMS

To measure the microstrains, several strain gauges are used. These strain gauges are arranged to measure the microstrains in all directions. The arrangement of strain gauges for both the bigger and the smaller specimens is shown in Fig. 2. Moreover, four displacement transducers are applied to measure both the longitudinal and the transverse displacements. In the experiment, a high stiffness testing machine is used, and the loading is continued until the longitudinal macrostrain attains a value of at least 1% .

4. PARAMETRIC STUDY

In the present study, the effect of the strength of mortar, size of specimens, and the measuring procedure (i.e. gauge length) on the microstrains are investigated. For this purpose, the specimens shown in Table 2 are classified into 3 groups A, B, and C. These groups are explained in Table 3.

Table 3. Classification of specimens

group	parameter	specimen no.
A	strength of mortar	(2 and 3) and (4 and 5)
B	size	(1 and 4)
C	gauge length	(1 and 2)

5. DISCUSSION ON THE RESULTS

5.1 DISTRIBUTION OF MICROSTRAINS

Since the main objective of this study is to measure the microstrains at different orientations, the specimens are designed to have different orientations which have both tensile and compressive microstrains. In the present study, from the geometry of specimens, the microstrains are observed at $\theta = 90^\circ$ which is expected to have the maximum tensile strain and at $\theta = 30^\circ$ and $\theta = 150^\circ$ which are expected to have compressive strains. However, if the geometry of the specimens is changed, the microstrains in other orientations can be measured. As shown in Figs.4 ~ 8, the distributions of the microstrains in the different directions are illustrated and compared with the calculated values through the assumption of the microplane models[2][3] for concrete. The calculated value can be expressed as follows:

$$\epsilon_n = \epsilon_{ij} n_i n_j \quad (1)$$

where ϵ_{ij} represents the macrostrain tensor and n is the direction cosine of the contact normal, $n=(\cos\theta, \sin\theta)$. θ is measured from the direction of the applied load to the contact normal as shown in Fig.3. According to the results, the effects of the measuring procedure(i.e. gauge length), mortar strength, and the size of specimens on the microstrain are observed as follows:

Effect of gauge length: From Figs.4 and 5, it can be seen that as the gauge length increases, the measured values of microstrains decrease. This is because the longer gauge measures the average strain between mortar and steel cylinders, while the shorter one measures the strain of mortar only which is expected to be higher than the average one. Moreover, as shown in Fig.4 (the case of shorter gauge), for $\theta = 30^\circ$ and $\theta = 150^\circ$, in the beginning the calculated microstrains using eq.(1) are overestimated, and then, after certain values of the applied macrostrain (for $\theta = 30^\circ$, $\epsilon_{11} = -0.50 \times 10^{-2}$ and for $\theta = 150^\circ$, $\epsilon_{11} = -0.35 \times 10^{-2}$), the calculated values are in between the maximum and the minimum observed values. On the other hand, as shown in Fig.5(the case of longer gauge), in the same directions of $\theta = 30^\circ$ and $\theta = 150^\circ$, the calculated values are always overestimated. For $\theta = 90^\circ$, as shown in Figs.4 and 5, the calculated microstrains are mostly in between the maximum and the minimum observed microstrains.

Effect of mortar strength: As shown in Figs.7 and 8, although two different mortar strengths are used, a minor differences of the microstrains are observed. This means that the behavior of the microstructure for different mortar strengths is almost similar to each other. Also, as can be seen in Figs.7 and 8, for $\theta = 30^\circ$ and $\theta = 150^\circ$, the calculated microstrains are overestimated until the value of $\epsilon_{11} = -0.20 \times 10^{-2}$ (ϵ_{11} is the applied macrostrain). After this value, the calculated microstrains are in between the maximum and the minimum observed values. For $\theta = 90^\circ$, almost the same tendencies between the calculated and the observed values are obtained.

Effect of size of specimens: As shown in Figs.4 and 7, higher values of microstrains are

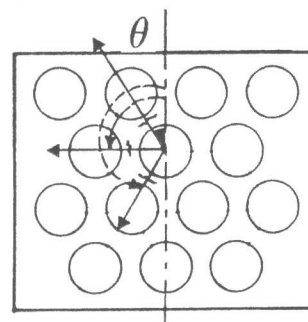


Fig. 3 Measurement of ' θ '

observed in the smaller size. This is due to the fact that the smaller size has less number of contacts which leads to more concentration of microstrains. On the other hand, in the case of big size, for the same loading conditions, the applied macrostrains will be distributed on larger number of contacts and less concentrations of microstrains will be observed.

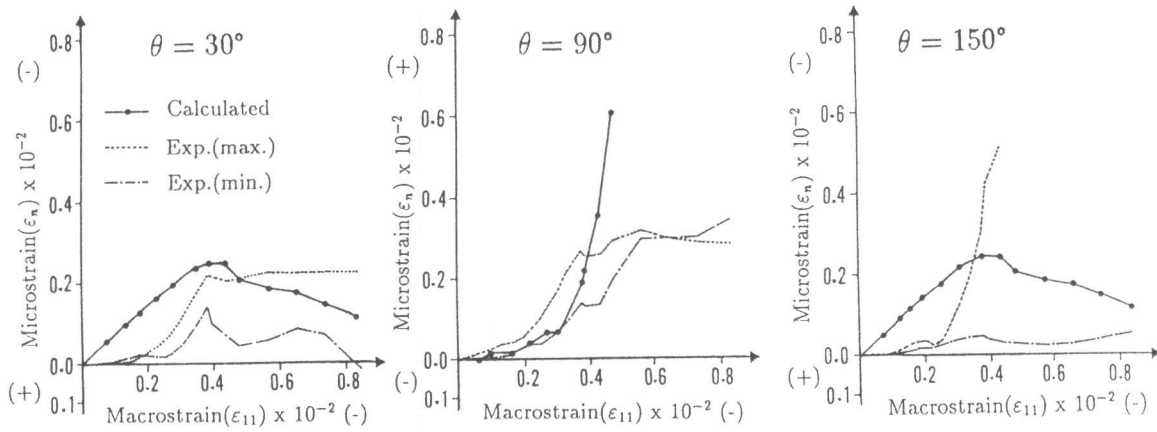


Fig. 4 Microstrain Distribution of Specimen no.(1)

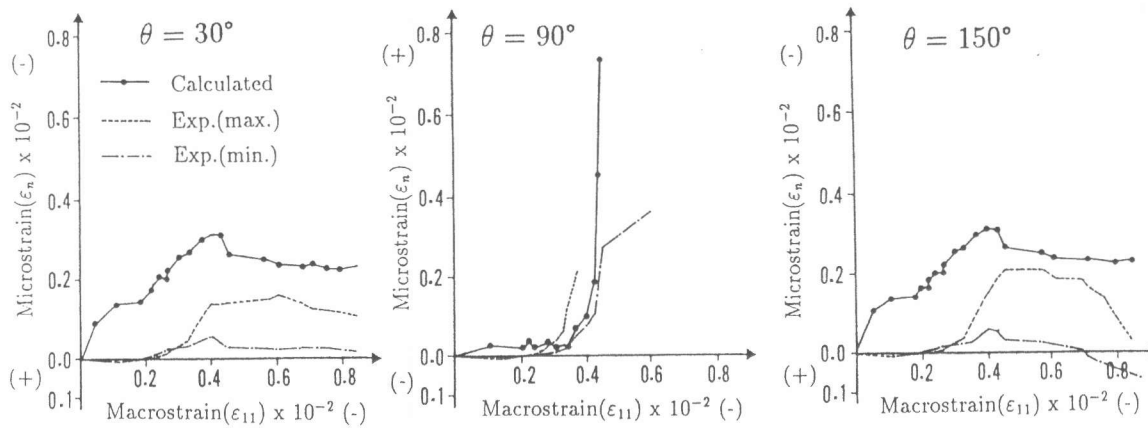


Fig. 5 Microstrain Distribution of Specimen no.(2)

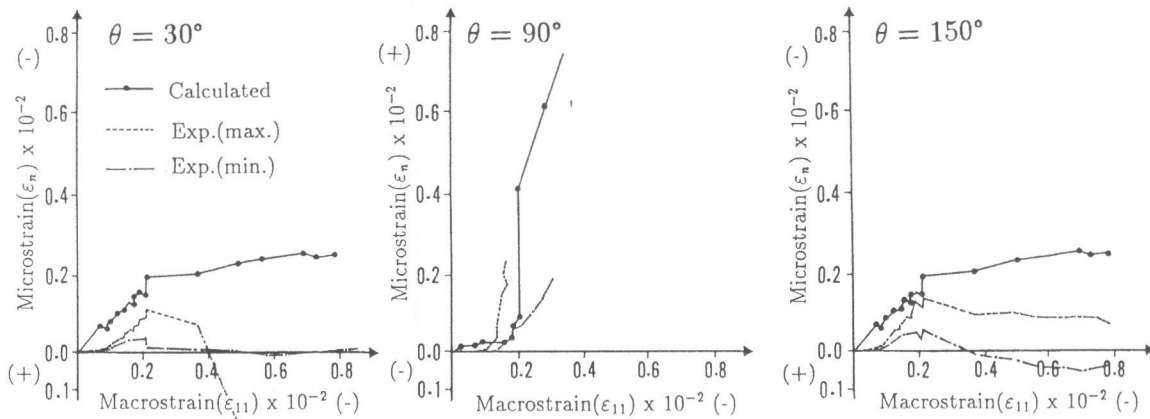


Fig. 6 Microstrain Distribution of Specimen no.(3)

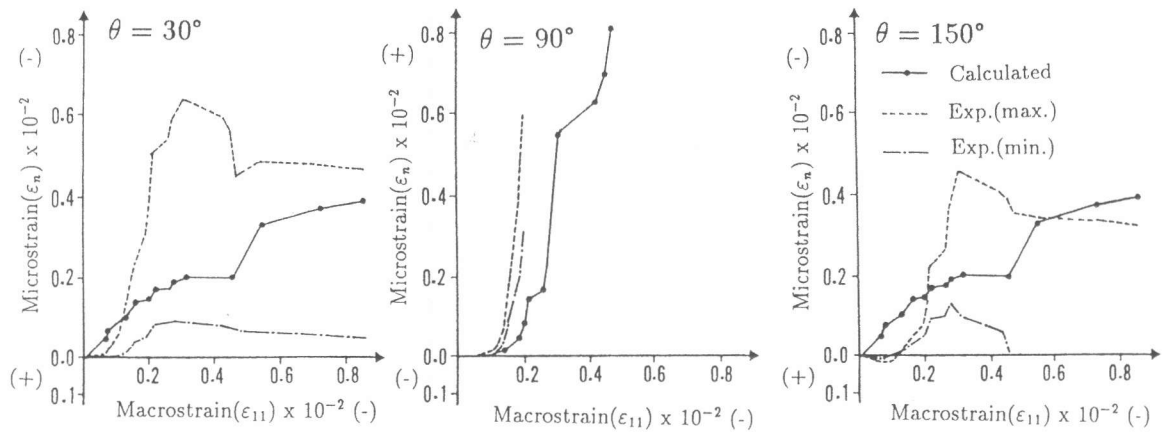


Fig. 7 Microstrain Distribution of Specimen no.(4)

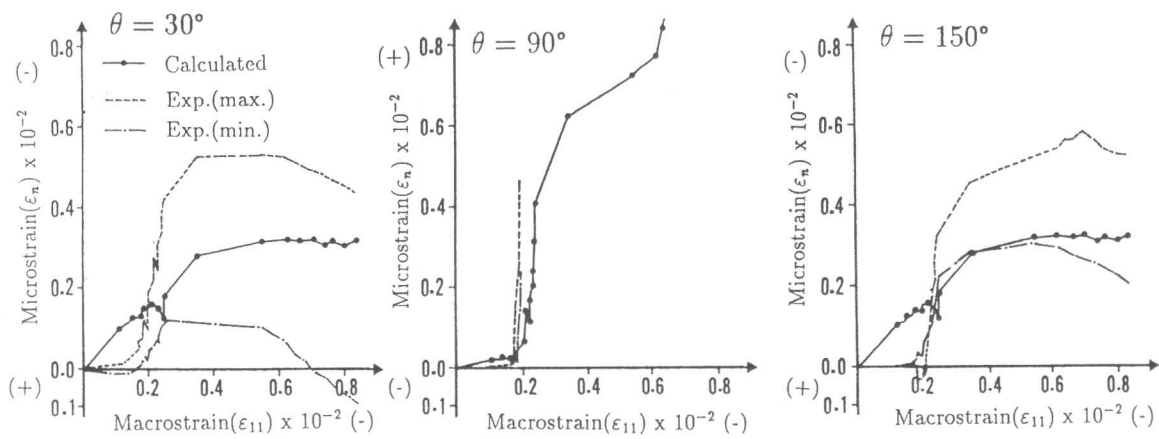


Fig. 8 Microstrain Distribution of Specimen no.(5)

5.2 CRACK PATTERNS

The crack patterns of all specimens are illustrated in Figs.9 and 10. It is observed that most of the cracks start either at the boundary of steel cylinders or in the thin layers of mortar located at the contacts. This means that the planes of weaknesses in concrete are not only at the thin layers of mortar located at the contacts as assumed by ref.[2] but also at the boundary of the coarse aggregate as proposed in ref.[3].

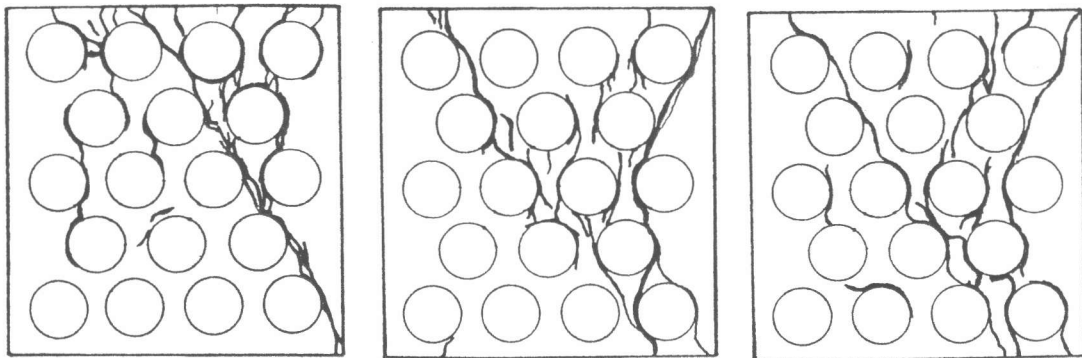


Fig. 9 Crack Patterns of Big Specimens

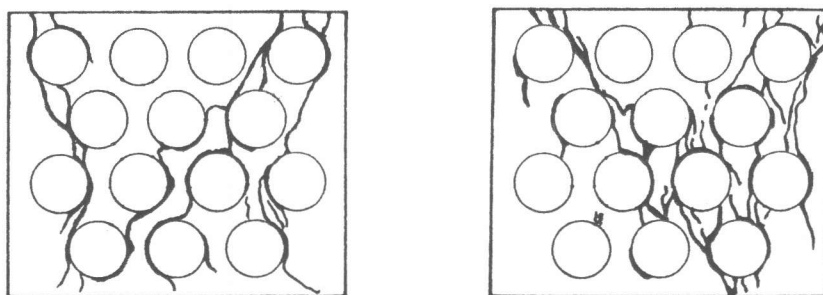


Fig. 10 Crack Patterns of Small Specimens .

6. CONCLUSIONS

In this study, an experimental work has been conducted microscopically for concrete. The first objective of the experiment is to observe the distribution of the microstrains at the contact. The second objective is to check whether concrete material is kinematically constrained or not. The effects of specimen size, strength of mortar, and gauge length on the strain distribution are investigated. It is observed that the microstrains are highly scattered, nonsmooth and cannot be predicted by a simple rule. It is recommended that the shorter gauge length should be used to measure the microstrains because it measures only the strains of mortar, while the measurements by the longer one is affected by the strains of the coarse aggregates. Also, it is noticed that minor differences of the microstrains are obtained with the use of different mortar strengths. Moreover, although a small variation of specimen sizes is used, an obvious difference of the microstrains is noticed. This is due to the fact that from the microscopic point of view, the behavior of the microstructure is greatly influenced by the quantity and the distribution of coarse aggregates. In addition, the crack patterns of all specimens are presented. It is observed that most of the cracks start either at the boundary of steel cylinders or in the thin layers of mortar located at the contacts. To have a general relationship between both the microscopic and macroscopic strains, a more comprehensive experimental work must be conducted on the microlevel. Moreover, the effect of mortar thickness at the contacts and the roughness of steel cylinders to consider the irregularity of aggregates on the microstrains should be observed. The authors are investigating the influence of these parameters and analytical proceedings show that these parameters have considerable bearing on the actual response.

REFERENCES

1. Batdorf, S. B., and Budiansky, B., "A Mathematical Theory of Plasticity Based on the Concept of Slip," NACA TN1871, April, 1949.
2. Bazant, Z. P. and Oh, A. M., "Microplane Model for Progressive Fracture of Concrete and Rock," *Journal of Engineering Mechanics*, ASCE, Vol. 111, No.4, April 1985, pp. 559-582.
3. Farahat, A. M., Wu, Z. S. and Tanabe, T., "Development of Microplane Model of Concrete with Plural Types of Granular Particles," *Proceeding of JSCE*, 1991-08, No. 433, Vol. 15, pp. 231-238.